

Accepted Manuscript

Evaluation of biological properties of 3,3',4,4'-benzophenonetetracarboxylic dianhydride derivatives and their ability to inhibit hexokinase activity

Krzysztof Kochel, Mateusz D. Tomczyk, Rui F. Simões, Tomasz Fraczek, Adrian Sobon, Paulo J. Oliveira, Krzysztof Z. Walczak, Aneta Koceva-Chyla

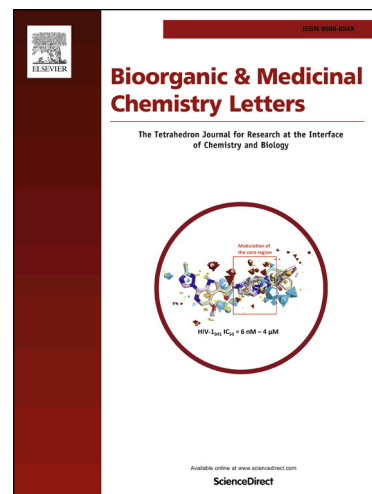
PII: S0960-894X(16)31334-8
DOI: <http://dx.doi.org/10.1016/j.bmcl.2016.12.055>
Reference: BMCL 24544

To appear in: *Bioorganic & Medicinal Chemistry Letters*

Received Date: 16 August 2016
Revised Date: 17 December 2016
Accepted Date: 20 December 2016

Please cite this article as: Kochel, K., Tomczyk, M.D., Simões, R.F., Fraczek, T., Sobon, A., Oliveira, P.J., Walczak, K.Z., Koceva-Chyla, A., Evaluation of biological properties of 3,3',4,4'-benzophenonetetracarboxylic dianhydride derivatives and their ability to inhibit hexokinase activity, *Bioorganic & Medicinal Chemistry Letters* (2016), doi: <http://dx.doi.org/10.1016/j.bmcl.2016.12.055>

This is a PDF file of an unedited manuscript that has been accepted for publication. As a service to our customers we are providing this early version of the manuscript. The manuscript will undergo copyediting, typesetting, and review of the resulting proof before it is published in its final form. Please note that during the production process errors may be discovered which could affect the content, and all legal disclaimers that apply to the journal pertain.



Evaluation of biological properties of 3,3',4,4'-benzophenonetetracarboxylic dianhydride derivatives and their ability to inhibit hexokinase activity

Krzysztof Kochel^{a,*}, Mateusz D. Tomczyk^b, Rui F. Simões^c, Tomasz Fraczek^d, Adrian Sobon^e, Paulo J. Oliveira^c, Krzysztof Z. Walczak^b, Aneta Koceva-Chyla^a

^aDepartment of Medical Biophysics, Faculty of Biology and Environmental Protection, University of Lodz, Pomorska 141/143, 90-236 Lodz, Poland

^bDepartment of Organic Chemistry, Bioorganic Chemistry and Biotechnology, Silesian University of Technology, Krzywoustego 4, 44-100 Gliwice, Poland

^cCNC - Center for Neuroscience and Cell Biology, University of Coimbra, UC-Biotech, Biocant Park, 3060-197 Cantanhede, Portugal

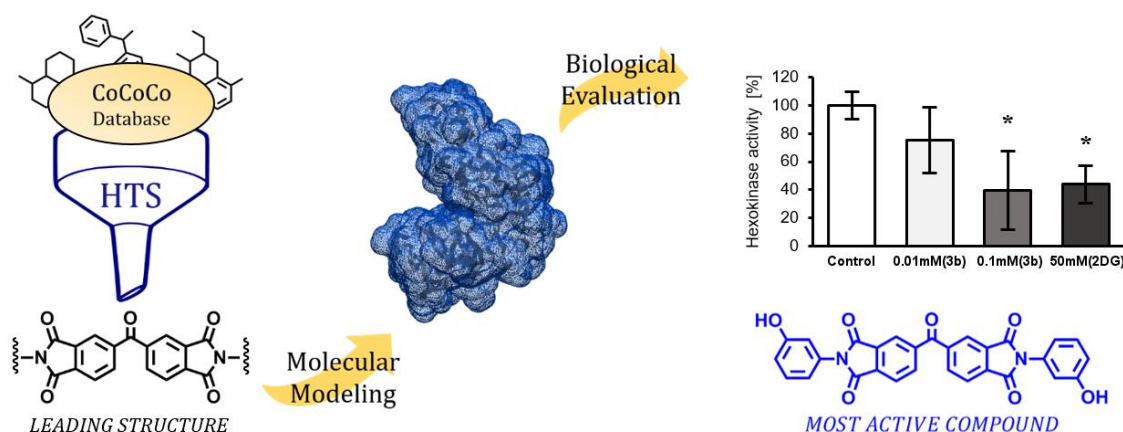
^dInstitute of Applied Radiation Chemistry, Faculty of Chemistry, Lodz University of Technology, Zeromskiego 116, 90-924 Lodz, Poland

^eDepartment of Industrial Microbiology and Biotechnology, Institute of Microbiology, Biotechnology and Immunology, Faculty of Biology and Environmental Protection, University of Lodz, Banacha 12/16, 90-237 Lodz, Poland

Abstract

This investigation has explored the properties of 3,3',4,4'-benzophenonetetracarboxylic dianhydride (BDTA) derivatives with regard to their being prospective inhibitors of hexokinase II (HKII). A pluripotent embryonic carcinoma cell line P19 (ECC), was used as the biological target for newly generated potential inhibitors of HKII. The results obtained from Virtual High-Throughput Study (VHTS), molecular modeling and biological activity studies showed BDTA to be a promising leading structure with a good binding score and simplest functionalization. The inhibitory effect was measured after 72 h incubation. Of selected BDTA derivatives, the most active was compound 3b, containing 3-hydroxyphenyl moiety in the para position, being able at 100 μ M to decrease the mass of differentiated P19dCs cells by 30%, changing both the mitochondrial transmembrane potential and $O_2^{\cdot-}$ level. Under these conditions, only compound 3b had the ability to decrease hexokinase activity in a dose-dependent manner.

Graphical abstract



Abbreviations: 3,3',4,4'-benzophenonetetracarboxylic dianhydride (BDTA); Embryonal carcinoma cells (ECC); Glukokinase (GK); Glucose 6-phosphate (G6P); Glucose 6-phosphate dehydrogenase (G6PD); Mitochondrial Membrane Potential (MMP); Mitochondrial Permeability Transition Pore (mPTP); Superoxide Anion ($O_2^{\cdot-}$); Sulforhodamine B (SRB); Tetramethylrhodamine (TMRE); Tricarboxylic acid (TCA); Virtual High-Throughput Study (VHTS); Voltage Dependent Anion Channel (VDAC).

Glycolysis, a metabolic process converting glucose into pyruvate, takes place in the cytosol and can proceed under both aerobic and anaerobic conditions. In eukaryotic cells, pyruvate enters the mitochondria matrix where it undergoes oxidation in the TCA cycle and contributions to oxidative phosphorylation and ATP synthesis. While normal cells almost exclusively use oxidative phosphorylation for the ATP synthesis, cancer cells, especially those in the rapidly growing tumors with high demand for glucose, increase the level of aerobic glycolysis, from respiration towards fermentation that generates lactate even in aerobic conditions¹. This specific metabolic pattern (Warburg effect²) ensures that substrates and more ATP are produced for rapidly proliferating cancer cells¹. High level of aerobic glycolysis aids malignant cell survival in a hypoxic or acidosis microenvironment during the development of a cancer. Many normal cells, ranging from microbes to lymphocytes, also use aerobic glycolysis during increased proliferation, suggesting that this process meets the metabolic requirements of rapidly dividing cells and support their growth³³.

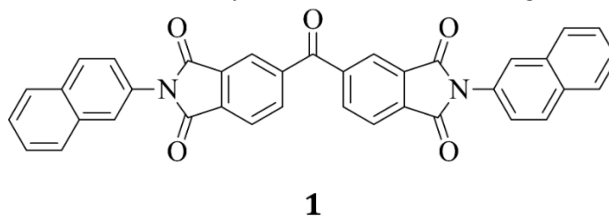
Glucose metabolism starts with phosphorylation of its 6-hydroxyl group⁴, trapping G6P inside the cell. The process is catalyzed by hexokinases, a family with 4 isoforms (HKI, HKII, HKIII and HKIV) showing cell- and tissue-specific expression, *e.g.* HKII mRNA expression can be up to 100-fold higher in cancer cells than normal cells⁵. HKs I-III are widely distributed in mammalian tissues, whereas HKIV, a specific isoform of hexokinase (also known as GK) is mainly expressed in liver and pancreatic β -cells^{4,6}. GK structure contains only one 50 kDa domain, whereas other HKs have two 50 kDa domains. Unlike other hexokinase isoforms, capable of phosphorylating several hexoses, GK have a 50-fold lower affinity for its substrate, which is only glucose⁷. The two most common isoforms HKI and HKII overlap in tissue expression, but they have different subcellular distributions; their N-terminal domains allow them to attach to the outer membrane of mitochondria⁴. Whereas HKI is mainly associated with mitochondria, HKII is associated with both mitochondrial and cytoplasmic compartments. It has been postulated that the differences in the subcellular distribution of HKI and HKII isoforms might result in different metabolic roles in cells. Mitochondrially-bound HKs may direct the catabolism of glucose (G6P formation towards glycolysis), whereas cytoplasmic HKII may control its anabolism (glycogen synthesis)⁸. Indeed, the catabolic and anabolic fates of glucose are dynamically regulated by its extracellular fraction.

Regulation of HKII activity and its subcellular translocation involves the participation of intracellular glucose, G6P and Akt, all acting as signaling molecules. The activity of HKI is much less sensitive to control by these factors, and this HK isoform is mainly committed to glycolysis. These processes could be important in HKs allowing cells to keep their energy balance, to adapt to changing metabolic conditions and in avoiding injury⁸.

Mitochondrial HKII is necessary for the survival of cancer cells⁵. In almost 70% of cells⁹, once HKII has been phosphorylated by Akt kinase, it binds to VDAC, a protein located in the outer mitochondrial membrane. HKII binding to VDAC stabilizes mPTP and inhibits apoptosis by blocking the pro-apoptotic activity of Bax and Bak proteins. The dual role of HKII in both processes, aerobic glycolysis and cell survival, makes this HK isoform an attractive subject for investigation^{9,10}. Research to date has resulted in the discovery of different molecules that can cleave mitochondrial HKII¹¹, found that it interacts with VDAC¹², and allosterically inhibits the cytosolic fraction of this enzyme¹³, thereby promoting cancer cell death. Glucosamine derivatives can also interact with the active center of HKII¹⁴.

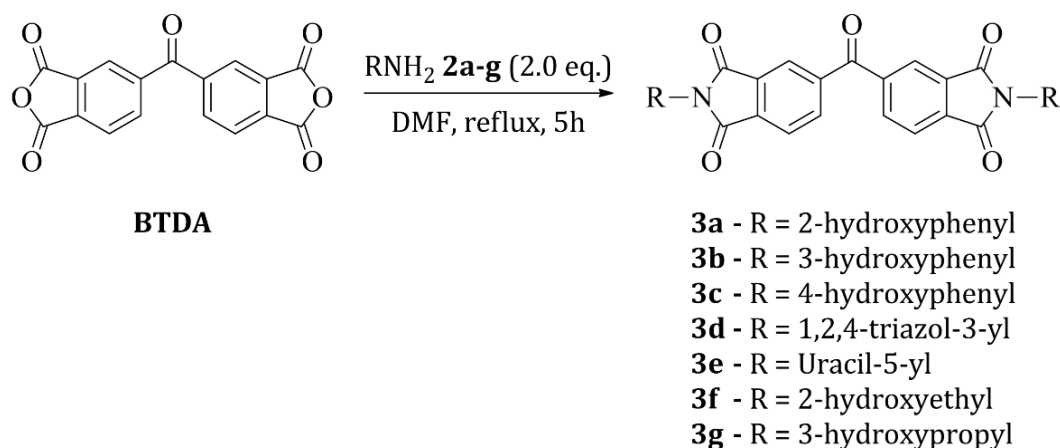
We have focused our investigation on BDTA derivatives as prospective inhibitors of HKs, which to the best of our knowledge has not been previously undertaken in the search for potential anticancer agents.

The chemical structures of the compounds, we selected for our investigation, have been examined by VHTS. The AutoDock Vina¹⁵, a chemical database downloaded from the Commercial Compound Collection¹⁶, was used for this purpose. The open form of HKII¹⁷ was chosen as a receptor model. From the results of the final analysis, compound **1** (Scheme 1) was selected as the most worthy structure for further investigation.



Scheme 1. Chemical structure of compound **1**.

Since compound **1** contains only hydrophobic naphthalene groups, we synthesized other derivatives, named **3a-g**, which include a hydroxyl group as a common structural element along with different structural variations, such as heterocyclic rings and flexible alkyl chains. The condensation reaction involved a 2-fold excess of amino compounds with respect to BTDA in polar aprotic solvent DMF (20 ml). The reaction was carried out in reflux, its progress being monitored by TLC (MeOH:CHCl₃, 1:1, v/v). When TLC indicated complete consumption of BTDA, the mixture was cooled and poured into the water. The precipitant was filtered off, rinsed with cold water and recrystallized twice from glacial acetic acid. The structure of synthesized compounds was based on analytical data from ¹H NMR, ¹³C NMR, IR and MALDI TOF MS¹⁸.



Scheme 2. Synthesis of BDTA derivatives **3a-g**¹⁸.

To predict the binding mode of compounds **3a-g** with an open form of HKII¹⁷, a more detailed study was carried out by a molecular docking technique. The protein model was prepared in Protein Preparation Wizard. All small molecules (water, ATP and ions) were removed for clarity. Water was removed since there are no available data indicating its role in ligand binding within the enzyme. ATP was removed as it does not affect docking of our ligands. The receptor grid was centered at Asp657, the size of the receptor box was set at 10 Å. To model small changes in the receptor caused by ligand binding, van der Waals radii of amino acid residues were scaled down by 0.9. The results are presented in Table 1. The best docking score was with compound **3b**, and the weakest one was compound **3c**. Interestingly, the most active compound (**3b**) and the inactive compound (**3e**) had similar *e-model* value (one of the scoring functions used by Glide).

Table 1. Glide docking results for examined compounds

Compound	Docking score [kcal/mol]	<i>e-model</i>
3b	-6.3	-61.7
3g	-5.7	-54.2
3f	-5.6	-53.2
3a	-5.2	-56.1
3e	-4.9	-61.4
3d	-4.9	-48.5
3c	-4.7	-52.2

The predicted binding mode of **3b** is shown in Image 1. The ligand binds along the active site located in the deep cleft of the enzyme (1a). Compound **3b** forms 4 hydrogen bonds with Thr658, Asp861, Ser682 and Trp709, and has a π -cation interaction with Lys510. There was also some expected interactions between π electrons of one of phthalimide moieties with the carboxyl group of Asp657. The predicted binding mode of **3e** was different from that of **3b**, however, both compounds occupy roughly the same site on the enzyme. Moreover, **3b** and **3e** form a hydrogen bond with Asp861. In contrast, the cytotoxic compound **3d** is not so deeply buried in the binding site than the previously discussed compounds, possibly explaining its lack of activity with hexokinase (1c)¹⁹⁻²².

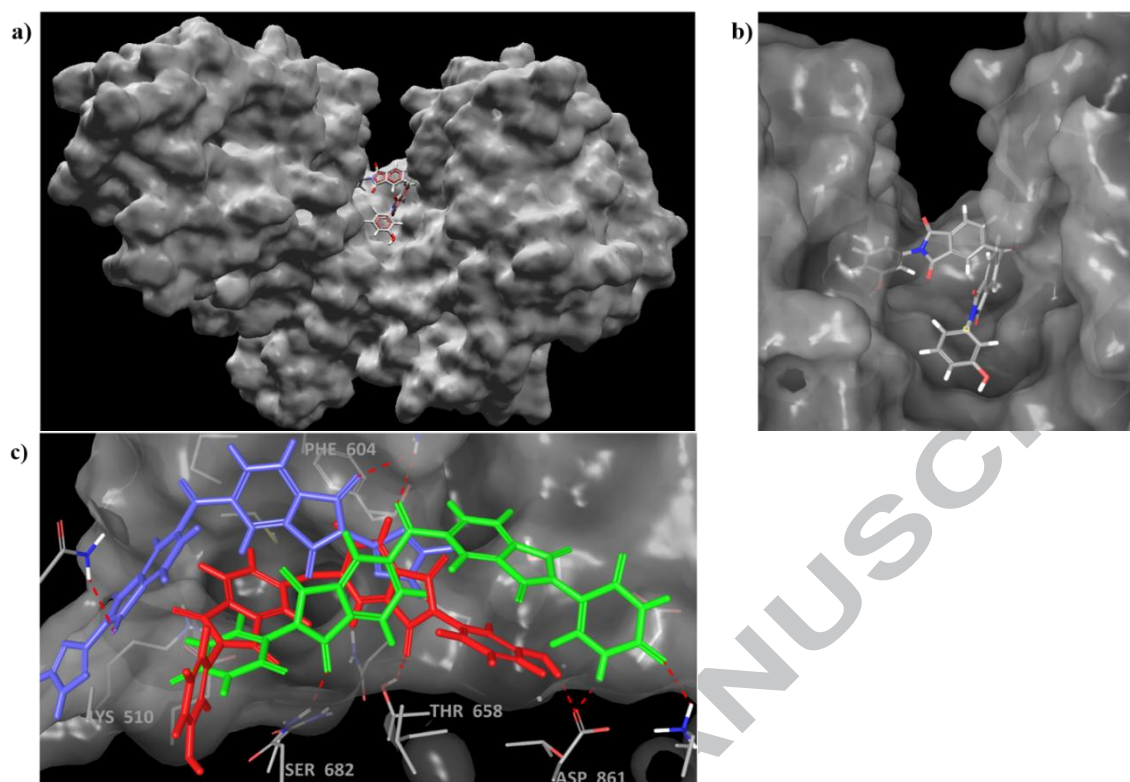


Image 1. BDTA derivative **3b** docked to HKII: a) whole enzyme, b) close-up of docking site. Overlay of predicted binding modes of BDTA derivatives (panel c): **3d** (blue) **3b** (red) and **3e** (green).

Cytotoxicity was assayed using P19 cells (CRL-1825; Manassas, VA, USA), which can be cultured in the undifferentiated (P19SCs) or differentiated state (P19dCs). P19SCs cells are highly glycolytic for energy production, have immature, poorly polarized and inactive mitochondria²³ and compared with P19dCs cells also have twice the level of mitochondrially-bound HKII, much higher lactate production and use 30% more glucose²³. Mitochondria of P19dCs cells are more polarized and filamentous²³.

Table 2. Effect of incubation time and concentration of BDTA derivatives on cell mass and metabolic activity. Data are means \pm SD from at least 4 independent measurements in 6 repeats of each. Bold values are statistically significant compared with the control ($p < 0.05$). Undifferentiated and differentiated P19 cells are described as P19SCs or P19dCs, respectively..

SRB assay						
Compound	P19SCs			P19dCs		
	24 h	48 h	72 h	24 h	48 h	72 h
2	120.4 \pm 22.5	99.6 \pm 4.1	103.8 \pm 8.0	90.5 \pm 13.7	93.6 \pm 7.5	97.4 \pm 9.5
3a	103.6 \pm 1.9	102.0 \pm 7.9	106.5 \pm 10.2	95.6 \pm 16.4	93.0 \pm 17.8	79.8 \pm 4.2
3b	103.3 \pm 12.4	79.9 \pm 14.1	58.9 \pm 16.0	100.0 \pm 19.8	102.2 \pm 27.2	71.9 \pm 3.3
3c	90.2 \pm 6.6	81.8 \pm 5.2	86.8 \pm 2.6	86.7 \pm 22.1	48.5 \pm 13.0	30.9 \pm 4.3
3d	81.2 \pm 9.3	77.6 \pm 9.4	45.5 \pm 15.8	93.3 \pm 6.1	96.0 \pm 2.2	82.0 \pm 12.1
3e	115.2 \pm 11.2	99.4 \pm 6.8	97.4 \pm 11.1	95.8 \pm 19.4	88.2 \pm 15.1	90.8 \pm 18.6
3f	83.9 \pm 15.8	92.4 \pm 9.3	106.7 \pm 7.9	96.2 \pm 7.3	108.4 \pm 7.4	80.5 \pm 15.4
3g	106.0 \pm 9.8	101.5 \pm 2.0	100.0 \pm 2.5	110.6 \pm 0.7	97.9 \pm 7.4	94.7 \pm 3.2

Resazurin assay						
2	100.1 \pm 6.0	91.2 \pm 10.1	101.3 \pm 4.1	90.5 \pm 1.4	101.7 \pm 3.9	94.4 \pm 7.5
3a	103.5 \pm 4.6	99.7 \pm 5.4	101.2 \pm 6.9	105.0 \pm 9.0	105.3 \pm 2.9	99.4 \pm 3.2
3b	102.6 \pm 8.2	76.5 \pm 5.7	59.8 \pm 17.5	100.0 \pm 11.3	97.5 \pm 15.2	91.5 \pm 7.2
3c	88.5 \pm 4.4	74.4 \pm 2.7	79.9 \pm 4.0	96.2 \pm 2.6	87.4 \pm 2.3	93.8 \pm 2.2
3d	92.7 \pm 19.6	94.0 \pm 4.4	53.2 \pm 23.7	114.0 \pm 18.4	96.1 \pm 21.0	86.5 \pm 29.7
3e	113.8 \pm 10.6	103.2 \pm 10.3	109.6 \pm 10.3	116.3 \pm 15.1	105.3 \pm 7.2	105.0 \pm 12.0
3f	101.5 \pm 1.2	107.8 \pm 6.4	113.8 \pm 10.2	113.3 \pm 14.3	103.7 \pm 5.3	99.4 \pm 14.5
3g	105.0 \pm 4.8	98.1 \pm 4.1	100.0 \pm 2.3	100.1 \pm 4.0	101.1 \pm 0.4	98.1 \pm 1.3

Cytotoxicity in both types of cells was estimated after incubation with 1, 10, or 100 μM of **3a-g** for 24, 48 or 72 h in culture, and subsequent analysis involved SRB²⁴ and resazurin²⁵ assays. The metabolic activity of cells was measured by the resazurin assay, and their mass by the SRB technique. None of the compounds were cytotoxic at 1 and 10 μM concentrations. At 100 μM the highest activity was with compounds **3b** and **3d**, and the longer incubation time of 72 h increased cytotoxicity assayed with SRB method. Both compounds acted more potently on P19SCs cells than P19dCs cells. In contrast, compound **3c** containing a hydroxyl group in the para position of the benzene ring was more effective on the differentiated cells, decreasing their mass by 70%. Compounds **3f** and **3g** with an aliphatic chain at the nitrogen atom of imide skeleton instead of a phenol group were inactive (Table 2).

Based on cytotoxicity results, we selected compounds **3a**, **3b** and **3c** to examine the changes in the MMP and mitochondrial $\text{O}_2^{\cdot-}$ level in P19 cells, using TMRE²⁶ and MitoSox²⁷ fluorescent dyes. Cells were incubated for 24 h or 72 h with 1 or 100 μM of each compound and the results are given in Table 3.

Compound **3a** was inactive on both cell types. Compound **3b** decreased metabolic activity and mass of both cell lines, but only after the longer incubation time (72 h). Literature data show that HKII can regulate MMP and ROS production²⁸. Thus, we decided to investigate whether selected BDTA derivatives influence on MMP and ROS level. Compound **3b** increased MMP in P19SCs cells, but had the opposite effect on P19dCs cells. A 24 h incubation of the undifferentiated cells with compound **3c**, irrespective of its concentration, significantly increased MMP. Under the same conditions, differentiated cells behaved differently, but a decrease in the MMP occurred in cells incubated at 100 μM .

The mitochondrial $\text{O}_2^{\cdot-}$ level decreased in P19SCs incubated with 100 μM **3b** for 24 h, but increased in cells incubated with 1 or 100 μM **3a** for 72 h. P19dCs cells incubated with 1 or 100 μM **3c** for 72 h showed an increase in the MMP.

Table 3. Effect of incubation time and concentration of 3b, 3c and 3d on MMP and mitochondrial $\text{O}_2^{\cdot-}$. Data are means \pm SD from 4 independent measurements in at least 4 repeats of each. Bold values are statistically significant compared with the control ($p < 0.05$). P19 undifferentiated and differentiated cells are called P19SCs or P19dCs, respectively.

Compound	MMP							
	P19SCs				P19dCs			
	24 h		72 h		24 h		72 h	
	1 μM	100 μM	1 μM	100 μM	1 μM	100 μM	1 μM	100 μM
3a	82.2\pm13.6	89.6 \pm 19.1	81.9 \pm 21.9	81.6 \pm 14.9	117.8 \pm 12.7	112.0 \pm 10.2	89.40 \pm 16.3	93.3 \pm 11.1
3b	86.0 \pm 18.7	91.0 \pm 21.0	110.4 \pm 12.6	131.1\pm18.9	94.5 \pm 18.6	96.4 \pm 15.2	87.8 \pm 8.0	50.9\pm16.4
3c	176.1\pm16.3	206.6\pm15.2	93.0 \pm 8.7	116.7\pm17.2	110.6 \pm 12.2	65.8\pm15.6	144.7 \pm 29.1	136.6 \pm 11.1

Compound	Mitochondrial $\text{O}_2^{\cdot-}$ level							
	P19SCs				P19dCs			
	24 h		72 h		24 h		72 h	
	1 μM	100 μM	1 μM	100 μM	1 μM	100 μM	1 μM	100 μM
3a	108.7 \pm 37.0	108.3 \pm 39.8	115.4\pm33.6	129.9\pm24.0	111.1 \pm 39.2	168.0 \pm 39.5	97.8 \pm 35.0	86.0 \pm 24.2
3b	83.2 \pm 36.9	55.1\pm39.8	106.0 \pm 22.1	108.3 \pm 34.7	112.2 \pm 39.5	117.4 \pm 40.9	105.3 \pm 16.7	149.1\pm38.4
3c	72.1 \pm 32.0	106.6 \pm 24.6	78.4 \pm 36.4	72.5 \pm 39.7	75.8 \pm 33.0	113.2 \pm 27.6	138.0\pm22.3	118.8 \pm 22.2

The inhibitory effect of these compounds on hexokinase activity was measured spectrophotometrically in cell lysates by following an increase in NADPH absorbance at 340 nm²⁹. As a positive control a pure enzyme (HKII, 6308-100 from BioVision) was used. Parameters of its kinetic are given in Table 4. Results for K_m are different from those reported in the literature. Ardehali et al.,^{30,31} got K_m values of 0.34 ± 0.06 and 0.36 ± 0.10 , whereas Ahn et al.,³² got 0.37 ± 0.12 . These differences may result from slightly different methods and enzyme sources used to determine K_m . The first values were determined by measuring the phosphorylation of [^{14}C]-labeled glucose as a function of glucose added to the reaction mixture. The second method was based on spectrophotometric measurement in which G6P formation is coupled with the NADPH production in the presence of an excess of G6PD. Under these conditions only compound **3b** decreased hexokinase activity in a dose-dependent manner (Figs 1 and 2).

Table 4. Kinetic parameters of HKII enzyme monitored at 340 nm. The results, shown as means \pm SD, are from 4 independent experiments in at least 4 repeats of each.

K_m (glucose)	V_{max}	k_{cat}	K_{cat}/K_m
[mM]	[mM min ⁻¹]	[sec ⁻¹]	[M ⁻¹ s ⁻¹]
0.42 \pm 0.07	0.016 \pm 0.004	93.39 \pm 23.38	0.22*10 ⁶

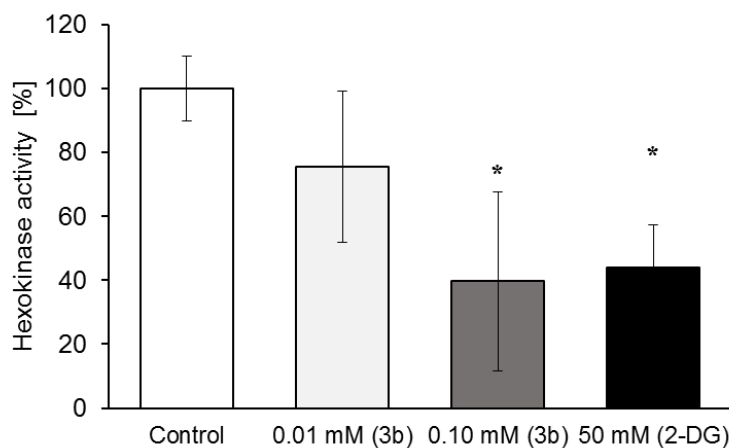


Fig. 1. Effect of **3b** and **2-DG** on hexokinase activity in supernatant of freshly prepared lysates of P19SCs cells. The results, shown as means \pm SD, are from 4 independent experiments in at least 4 repeats of each. * $p < 0.05$ - statistically significant in relation to control.

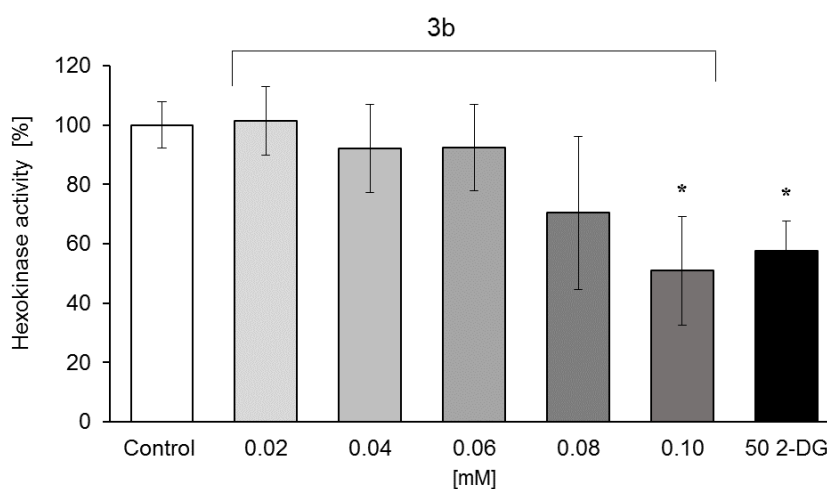


Fig. 2. Effect of **3b** and **2-DG** on the activity of HKII (Recombinant human hexokinase II protein, 6308-100 from BioVision). The results, shown as means \pm SD, are from 4 independent experiments in at least 4 repeats of each. * $p < 0.05$ - statistically significant in relation to control.

Summarizing, in examining the biological activity of BDTA derivatives and their ability to inhibit hexokinase activity, our results indicate that the compounds with a hydroxybenzene ring were cytotoxic to mouse embryonic carcinoma cells, but only at relatively high concentrations. Among newly synthesized BDTA derivatives only **3b** compound was able to partially inhibit a HK activity at a concentration at least 500 times lower (100 μ M) than 2-DG (50 mM). This demonstrates that compound **3b** can be considered as a core structure in the design and development of novel and effective hexokinase inhibitors.

References and notes

- Lincet, H.; Icard, P. *Oncogene* **2015**, *34*, 3751–3759.
- Warburg, O. *Science (80-)*. **1956**, *123*, 309–314.
- Lunt, S. Y.; Vander Heiden, M. G. *Annu. Rev. Cell Dev. Biol.* **2011**, *27*, 441–464.
- Wilson, J. E. *J. Exp. Biol.* **2003**, *206*, 2049–2057.
- Mathupala, S. P.; Ko, Y. H.; Pedersen, P. L. *Semin. Cancer Biol.* **2009**, *19*, 17–24.
- Meglsson, M. D.; Matschinsky, F. M. *Diabetes / Metab. Rev.* **1986**, *2*, 163–214.
- Printz, R. L.; Magnuson, M. A.; Granner, D. K. *Annu. Rev. Nutr.* **1993**, *13*, 463–496.
- John, S.; Weiss, J. N.; Ribalet, B. *PLoS One* **2011**, *6*, e17674.
- Shoshan-Barmatz, V.; Zakar, M.; Rosenthal, K.; Abu-Hamad, S. *Biochim. Biophys. Acta - Bioenerg.* **2009**, *1787*, 421–430.
- Majewski, N.; Nogueira, V.; Bhaskar, P.; Coy, P. E.; Skeen, J. E.; Gottlob, K.; Chandel, N. S.; Thompson, C. B.; Robey, R. B.; Hay, N. *Mol. Cell* **2004**, *16*, 819–830.
- Goldin, N.; Arzoine, L.; Heyfets, A.; Israelson, A.; Zaslavsky, Z.; Bravman, T.; Bronner, V.; Notcovich, A.; Shoshan-Barmatz, V.; Fleischer, E. *Oncogene* **2008**, *27*, 4636–4643.
- Li, Y. C.; Fung, K. P.; Kwok, T. T.; Lee, C. Y.; Suen, Y. K.; Kong, S. K. *Life Sci.* **2002**, *71*, 2729–2740.
- Pelicano, H.; Martin, D. S.; Xu, R.-H.; Huang, P. *Oncogene* **2006**, *25*, 4633–46.
- Lin, H.; Zeng, J.; Xie, R.; Schulz, M. J.; Tedesco, R.; Qu, J.; Erhard, K. F.; Mack, J. F.; Raha, K.; Rendina, A. R.; Szewczuk, L. M.; Kratz, P. M.; Jurewicz, A. J.; Cecconie, T.; Martens, S.; McDevitt, P. J.; Martin, J. D.; Chen, S. B.; Jiang, Y.; Nickels, L.; Schwartz, B. J.; Smallwood, A.; Zhao, B.; Campobasso, N.; Qian, Y.; Briand, J.; Rominger, C. M.; Olejowski, C.; Hardwicke, M. A.; Luengo, J. I. *ACS Med. Chem. Lett.* **2016**, *7*, 217–222.
- Trott, O.; Olson, A. J. *J. Comput. Chem.* **2010**, *31*, 455–461.
- Del Rio, A.; Barbosa, A. J. M.; Caporuscio, F.; Mangiardi, G. F. *Mol. Biosyst.* **2010**, *6*, 2122.
- Schiani, B.; Rio, A. D.; Marini, C.; Sambucetti, G.; Cordera, R.; Maggi, D. *Endocr. Relat. Cancer* **2014**, *21*, R461–R471.
- All reagents and solvents were of analytical grade, obtained from commercial suppliers and used without further purification except for DMF, which was distilled prior to use and dried through storage over activated 4A molecular sieves. The progress of reaction was monitored by TLC using silica-gel-coated aluminium plates with a fluorescence indicator (SiO₂ 60, F254) and visualized by UV light. Column chromatography was performed using silica gelpacked columns (particle size 0.040-0.063 mm, Merck). ¹H NMR spectra were recorded on a Varian 600 MHz System or Agilent 400 MHz Spectrometer; ¹³C NMR spectra were recorded at 150 MHz or 100 MHz, respectively. Chemical shifts were measured relative to residual non-deuterated solvent resonances. Melting points were determined using a Boethius M HMK hot-stage apparatus. IR spectra (ATR technique) were recorded on Nicolet 6700 FT-IR Spectrometer (Thermo Scientific). MALDI TOF MS spectra were performed using a QTRAP 4500 Ab Sciex. N,N'-bis(2-hydroxyphenyl)benzophenone-3,3',4,4'-tetracarboxylic diimide (3a) As light yellow solid in 89%. m.p. >300 °C. ¹H NMR (400 MHz, DMSO-d₆): δ 6.94-6.96 (m, 2H), 7.00-7.03 (m, 2H), 7.28-7.36 (m, 4H), 8.17-8.21 (m, 4H), 8.27-8.29 (m, 2H), 9.89 (s, 2H). FT-IR (cm⁻¹): 3370 (m, br), 1780 (w), 1699 (s), 1389 (s), 717 (m). MALDI-TOF/MS (m/z): calc. for C₂₉H₁₆N₂O₇ 504.5, found 505.4 [M+H]⁺. N,N'-bis(3-hydroxyphenyl)benzophenone-3,3',4,4'-tetracarboxylic diimide (3b) As light yellow solid in 90%. m.p. >300 °C. ¹H NMR (400 MHz, DMSO-d₆): δ 6.85-6.87 (m, 6H), 7.32-7.35 (m, 2H), 8.15-8.17 (m, 4H), 8.25-8.26 (m, 2H), 9.78 (s, 2H). FT-IR (cm⁻¹): 3300 (m, br), 1780 (w), 1718 (s), 1391 (s), 715 (m). MALDI-TOF/MS (m/z): calc. for C₂₉H₁₆N₂O₇ 504.5, found 505.4 [M+H]⁺. N,N'-bis(4-hydroxyphenyl)benzophenone-3,3',4,4'-tetracarboxylic diimide (3c) As light yellow solid in 94%. m.p. >300 °C. ¹H NMR (400 MHz, DMSO-d₆): δ 6.88-6.90 (d, 4H), 7.23-7.25 (d, 4H), 8.12-8.15 (m, 4H), 8.23-8.25 (m, 2H), 9.78 (s, 2H). FT-IR (cm⁻¹): 3451 (m, br), 1779 (w), 1709 (s), 1390 (s), 715 (m). MALDI-TOF/MS (m/z): calc. for C₂₉H₁₆N₂O₇ 504.5, found 505.3 [M+H]⁺. N,N'-bis(1,2,4-triazol-3-yl)benzophenone-3,3',4,4'-tetracarboxylic diimide (3d) As grey solid in 71%. m.p. >300 °C. ¹H NMR (400 MHz, DMSO-d₆): δ 8.19-8.21 (m, 2H), 8.23-8.25 (m, 2H), 8.29-8.31 (m, 2H), 8.77 (s, 2H). FT-IR (cm⁻¹): 3392 (w, br), 1790 (w), 1730 (s), 1374 (s), 719 (m). MALDI-TOF/MS (m/z): calc. for C₂₁H₁₀N₈O₅ 454.4, found 455.2 [M+H]⁺. N,N'-bis(uracil-5-yl)benzophenone-3,3',4,4'-tetracarboxylic diimide (3e) As pale yellow solid in 91%. m.p. >300 °C. ¹H NMR (400 MHz, DMSO-d₆): δ 7.89 (s, 2H), 8.17-8.21 (m, 4H), 8.27-8.29 (m, 2H), 11.40 (br, 2H), 11.63 (br, 2H). FT-IR (cm⁻¹): 3180 (s), 3160 (s), 1770 (w), 1715 (s), 1385 (s), 745 (m). MALDI-TOF/MS (m/z): calc. for C₂₁H₁₆N₂O₇ 540.4, found 541.1 [M+H]⁺. N,N'-bis(2-hydroxyethyl)benzophenone-3,3',4,4'-tetracarboxylic diimide (3f) As pale grey solid in 89%. m.p. 208 °C. ¹H NMR (400 MHz, DMSO-d₆): δ 3.63 (q, J = 6.6 Hz, 4H), 4.13 (t, J = 6.6 Hz, 4H), 4.81 (br s, 2H), 8.17-8.20 (m, 4H), 8.27-8.29 (m, 2H). FT-IR (cm⁻¹): 3250 (w, br), 2954 (w), 1780 (w), 1714 (s), 1388 (s), 740 (m). MALDI-TOF/MS (m/z): calc. for C₂₁H₁₆N₂O₇ 408.4, found 409.5 [M+H]⁺. N,N'-bis(3-hydroxyprop-1-yl)benzophenone-3,3',4,4'-tetracarboxylic diimide (3g) As pale grey solid in 90%. m.p. 170 °C. ¹H NMR (400 MHz, DMSO-d₆): δ 1.76 (qt, J = 6.6 Hz, 4H), 3.46 (q, J = 6.6 Hz, 4H), 3.68 (t, J = 6.6 Hz, 4H), 4.51 (br s, 2H), 8.04-8.07 (m, 4H), 8.16-8.19 (m, 2H); FT-IR (cm⁻¹): 3242 (w, br), 2947 (w), 1779 (w), 1698 (s), 1393 (s), 743 (m). MALDI-TOF/MS (m/z): calc. for C₂₁H₁₆N₂O₇ 436.4, found 437.3 [M+H]⁺.
- Madhavi Sastry, G.; Adzhigirey, M.; Day, T.; Annabhimoju, R.; Sherman, W. *J. Comput. Aided. Mol. Des.* **2013**, *27*, 221–234.
- Friesner, R. A.; Banks, J. L.; Murphy, R. B.; Halgren, T. A.; Klicic, J. J.; Mainz, D. T.; Repasky, M. P.; Knoll, E. H.; Shelley, M.; Perry, J. K.; Shaw, D. E.; Francis, P.; Shenkin, P. S. *J. Med. Chem.* **2004**, *47*, 1739–1749.
- Friesner, R. A.; Murphy, R. B.; Repasky, M. P.; Frye, L. L.; Greenwood, J. R.; Halgren, T. A.; Sanschagrin, P. C.; Mainz, D. T. *J. Med. Chem.* **2006**, *49*, 6177–6196.
- Halgren, T. A.; Murphy, R. B.; Friesner, R. A.; Beard, H. S.; Frye, L. L.; Pollard, W. T.; Banks, J. L. *J. Med. Chem.* **2004**, *47*, 1750–1759.
- Vega-Naredo, I.; Loureiro, R.; Mesquita, K. A.; Barbosa, I. A.; Tavares, L. C.; Branco, A. F.; Erickson, J. R.; Holy, J.; Perkins, E. L.; Carvalho, R. A.; Oliveira, P. J. *Cell Death Differ.* **2014**, *21*, 1560–1574.
- Skehan, P.; Storeng, R.; Scudiero, D.; Monks, A.; McMahon, J.; Vistica, D.; Warren, J. T.; Bokesch, H.; Kenney, S.; Boyd, M. R. *JNCI J. Natl. Cancer Inst.* **1990**, *82*, 1107–1112.
- O'Brien, J.; Wilson, I.; Orton, T.; Pognan, F. *Eur. J. Biochem.* **2000**, *267*, 5421–5426.
- Rodrigues, E. T.; Pardo, M.; Laizé, V.; Cancela, M. L.; Oliveira, P. J.; Serafim, T. L. *Environ. Pollut.* **2015**, *206*, 619–626.
- Johnson-Cadwell, L. I.; Jekabsons, M. B.; Wang, A.; Polster, B. M.; Nicholls, D. G. *J. Neurochem.* **2007**, *101*, 1619–1631.
- da-Silva, W. S.; Gomez-Puyou, A.; de Gomez-Puyou, M. T.; Moreno-Sanchez, R.; De Felice, F. G.; de Meis, L.; Oliveira, M. F.; Galina, A. J. *Biol. Chem.* **2004**, *279*, 39846–39855.
- The 10 µl of supernatant of freshly prepared and centrifuged cell lysate or solution of HKII (Recombinant human Hexokinase II protein, 6308-100 from BioVision), was added to 88 µl of 100 mM Tris-HCl (pH 8.0) buffer containing 0.5 mM EDTA, 10 mM ATP, 10 mM MgCl₂, 2 mM glucose, 0.1 mM NADP (Sigma-Aldrich), and 0.1 U/ml of G6PD (Alfa-Aesar). HK activity was determined spectrophotometrically at 340 nm tracking the G6P-dependent conversion of NADP to NADPH. The reaction was initialized with 10 mM of ATP added to the reaction mixture after 10 min-preincubation of microplate at 37°C.

30. Ardehali, H.; Printz, R. L.; Whitesell, R. R.; May, J. M.; Granner, D. K. *J. Biol. Chem.* **1999**, *274*, 15986–15989.
31. Ardehali, H.; Yano, Y.; Printz, R. L.; Koch, S.; Whitesell, R. R.; May, J. M.; Granner, D. K. *J. Biol. Chem.* **1996**, *271*, 1849–1852.
32. Ahn, K.-J.; Kim, J.; Yun, M.; Park, J.-H.; Lee, J.-D. *BMB Rep.* **2009**, *42*, 350–355.

ACCEPTED MANUSCRIPT